Int. J. Heat Mass Transfer. Vol. 22, pp. 1567–1575.

0017–9310/79/1101–1567 $02.00/0

AN ANALYSIS OF THE EFFECT OF INLET SUBCOOLING ON CRITICAL HEAT FLUX OF FORCED CONVECTION BOILING IN VERTICAL UNIFORMLY HEATED TUBES

Y. KATTO
Department of Mechanical Engineering, University of Tokyo, Hongo, Bunkyo-ku, Tokyo, Japan

(*Received* 14 *December* 1978)

Abstract—In this paper, the generalized correlation of critical heat flux (CHF) derived by the author in previous studies is combined with the boiling length concept to make an analysis for obtaining theoretical predictions for the effect of inlet subcooling on CHF. Fairly good agreements are found between the theoretical predictions thus derived and the existing data of experiments. Then the extent of inlet subcooling over which the boiling length method is applicable for correlating CHF data is examined quantitatively by comparing the CHF data obtained in studies of so-called dryout and post-dryout heat transfer with the author's generalized correlation.

NOMENCLATURE

- d, I.D. of heated tube [m];
- G, mass velocity [kg m^{-2} s^{-1}];
- H_{fg}, latent heat of evaporation [J kg^{-1}];
- ΔH_i, inlet subcooling enthalpy [J kg^{-1}];
- K, dimensionless parameter for the effect of inlet subcooling, equation (1);
- l, length of heated tube [m];
- l_b, boiling length, equation (3) [m];
- M, $M = 0.0031 l/d$;
- N, $N = 107(\sigma\rho_l/G^2 l)^{0.54} l/d$;
- p, absolute pressure, Figs. 3–10 [bar];
- q_c, critical heat flux [W m^{-2}];
- q_{c0}, q_c for $\Delta H_i = 0$ [W m^{-2}];
- r, relative error, equations (9), (15) and (21);
- z, axial coordinate, Fig. 2 [m].

Greek symbols

- ε, $= (1/4)(d/l)(G\Delta H_i/q_c)$;
- ρ_l, density of liquid [kg m^{-3}];
- ρ_v, density of vapor [kg m^{-3}];
- σ, surface tension [N m^{-1}];
- χ, quality (χ_{ex}: exit quality corresponding to critical condition; χ_{in}: inlet quality).

1. INTRODUCTION

FOR CRITICAL heat flux (CHF) of forced convection boiling in vertical uniformly heated tubes, it is well known [1, 2] that plots of q_c against ΔH_i for fixed G often indicate the linear relationship such as is shown in Fig. 1, and it can be written as follows:

$$q_c = q_{c0}(1 + K\Delta H_i/H_{fg}), \tag{1}$$

where K is a dimensionless parameter independent of ΔH_i. Analyzing the experimental data of CHF, the author [3, 4] has shown that CHF data are classified into four regimes called L-, H-, N- and HP-regime. the linear equation (1) applies to regimes other than N-regime, and q_{c0} on the RHS of equation (1) is correlated by equations of the following form:

$$\frac{q_{c0}}{GH_{fg}} = f\left(\frac{\rho_v}{\rho_l}, \frac{\sigma\rho_l}{G^2 l}, \frac{l}{d}\right). \tag{2}$$

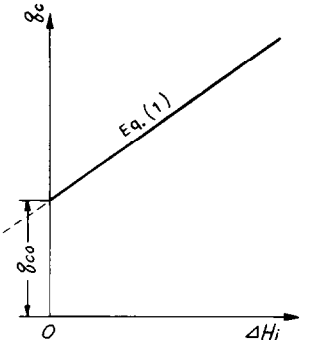

FIG. 1. Linear relationship between q_c and ΔH_i for fixed G.

On the other hand, the idea of the boiling length l_b indicated in Fig. 2(b), that is the tube length minus the length necessary to bring the thermodynamic quality to zero, was devised by Hewitt *et al.* [5] and Bertoletti *et al.* [6] for example, and has since come into use in correlating CHF data (e.g. GEXL correlation [7]). In the special case of $\Delta H_i < 0$ (that is, mixed inlet condition), the boiling length l_b can also be defined as indicated in Fig. 2(c). Then, for a uniformly heated tube, l_b is related to ΔH_i via the heat balance thus,

$$\frac{l_b}{l} = 1 - \varepsilon, \quad \text{where } \varepsilon = \frac{1}{4}\frac{d}{l}\frac{G\Delta H_i}{q_c}. \tag{3}$$

Equation (3) applies to both the case of Fig. 2(b) where $0 < \Delta H_i$ and that of Fig. 2(c) where $\Delta H_i < 0$.

Flow pattern at the point of reaching zero quality in Fig. 2(b) differs generally from that at the entrance of the heated tube in Fig. 2(a) where a saturated liquid is fed with no entrained vapor. However, in the case of $0 < \varepsilon \ll 1$ or $l_b/l = 1$ in equation (3), the boiling front

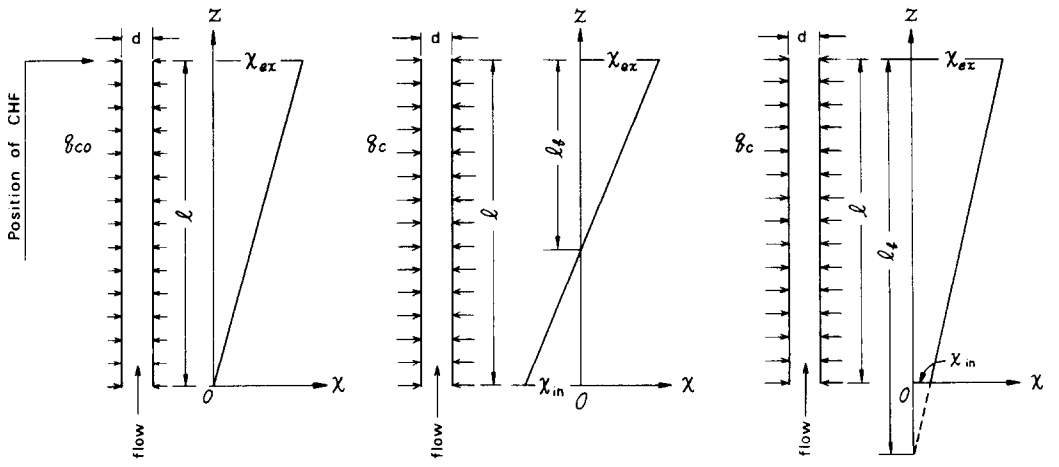

FIG. 2. Linear variation of quality χ along a uniformly heated tube.

can be approximately assumed to agree with the position of zero quality in Fig. 2(b). In other words, the CHF in this case can be correlated with the same function as equation (2), so that it is written as

$$\frac{q_c}{GH_{fg}} = f\left(\frac{\rho_v}{\rho_l}, \frac{\sigma\rho_l}{G^2 l_b}, \frac{l_b}{d}\right). \tag{4}$$

In the case of Fig. 2(c), the point of zero quality becomes an imaginary one, but if $l_b/l \doteqdot 1$, the same assumption of boiling front as above may be laid down without serious error.

Then, q_c in equation (1) with q_{c0} given by equation (2) should coincide with q_c in equation (4) with l_b given by equation (3), providing us with a means to discuss theoretically the parameter K on the RHS of equation (1).

2. PARAMETER K IN L-REGIME

According to the author's correlation of q_{c0} [3,4], equations (2) and (4) are written for L-regime as follows:

$$\frac{q_{c0}}{GH_{fg}} = C\left(\frac{\sigma\rho_l}{G^2 l}\right)^{0.043} \frac{1}{l/d} \tag{5}$$

$$\frac{q_c}{GH_{fg}} = C\left(\frac{\sigma\rho_l}{G^2 l_b}\right)^{0.043} \frac{1}{l_b/d}, \tag{6}$$

where $C = 0.34$ for both $\sigma\rho_l/G^2 l$ and $\sigma\rho_l/G^2 l_b < 5 \times 10^{-4}$, and $C = 0.25$ for both $\sigma\rho_l/G^2 l$ and $\sigma\rho_l/G^2 l_b > 5 \times 10^{-4}$. Then, dividing each member of equation (6) by that of equation (5), and substituting equation (3) for l_b, it yields the relation

$$q_c(1-\varepsilon)^{1.043} = q_{c0}. \tag{7}$$

When $|\varepsilon| < 1$, equation (7) can be expanded with respect to ε, and higher order terms than the second term can be ignored to give

$$q_c(1 - 1.043\varepsilon) = q_{c0} \tag{8}$$

with the relative error r defined as follows:

$$r = \frac{1 - 1.043\varepsilon}{(1-\varepsilon)^{1.043}} - 1. \tag{9}$$

Equation (9) indicates that the error can remain small for a comparatively wide range of ε. Then, replacing G included in ε of equation (8) by G of equation (5), it yields

$$q_c = q_{c0}\left\{1 + \frac{1.043}{4C(\sigma\rho_l/G^2 l)^{0.043}} \cdot \frac{\Delta H_i}{H_{fg}}\right\}.$$

Comparing this equation with equation (1), it gives K in L-regime (designated by K_L) as follows:

$$K_L = \frac{1.043}{4C(\sigma\rho_l/G^2 l)^{0.043}}, \tag{10}$$

where C takes the value indicated in equation (5).

In Fig. 3, K_L predicted by equation (10) is compared with the experimental data of K_L compiled in Fig. 16 of the preceding study [3]. Though data are limited in their number and show scattering, approximate agreement may be witnessed between predicted and measured K_L.

3. PARAMETER K IN H-REGIME

According to the author's correlation of q_{c0} [3], equations (2) and (4) are written for H-regime as follows:

$$\frac{q_{c0}}{GH_{fg}} = 0.10\left(\frac{\rho_v}{\rho_l}\right)^{0.133}\left(\frac{\sigma\rho_l}{G^2 l}\right)^{1/3} \frac{1}{1 + 0.0031 l/d} \tag{11}$$

$$\frac{q_c}{GH_{fg}} = 0.10\left(\frac{\rho_v}{\rho_l}\right)^{0.133}\left(\frac{\sigma\rho_l}{G^2 l_b}\right)^{1/3} \frac{1}{1 + 0.0031 l_b/d} \tag{12}$$

Dividing each member of equation (12) by that of

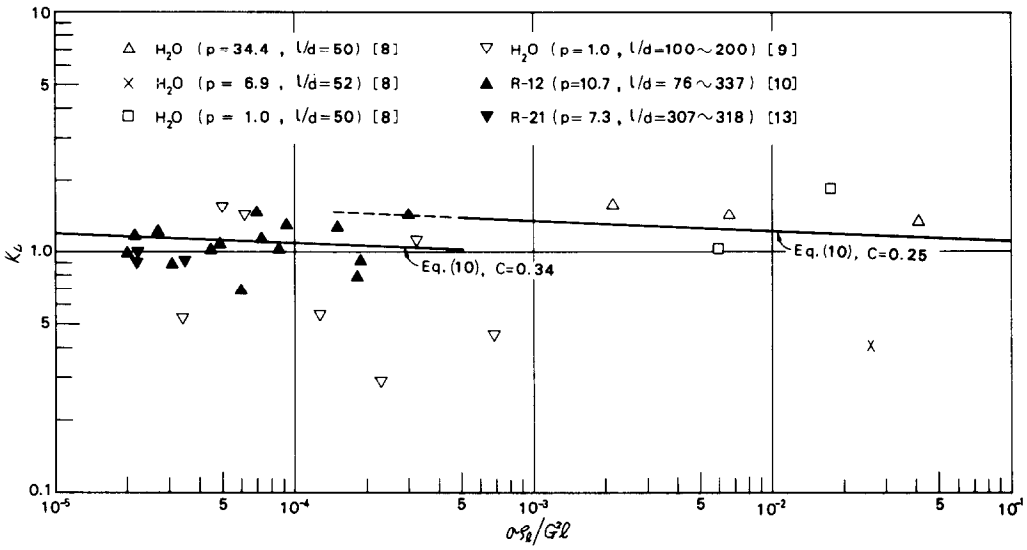

FIG. 3. Comparison between prediction of equation (10) and experimental data for K_L.

equation (11) and substituting equation (3) for l_b yields

$$q_c(1-\varepsilon)^{1/3}\frac{1+M(1-\varepsilon)}{1+M}=q_{c0}, \tag{13}$$

where $M=0.0031l/d$. When $|\varepsilon|<1$, equation (13) can be expanded with respect to ε, and higher order terms than the second term can be ignored to give

$$q_c\left\{1-\left(\frac{1}{3}+\frac{M}{1+M}\right)\varepsilon\right\}=q_{c0} \tag{14}$$

with the relative error r defined as follows:

$$r=\frac{1-\left(\frac{1}{3}+\frac{M}{1+M}\right)\varepsilon}{(1-\varepsilon)^{1/3}\dfrac{1+M(1-\varepsilon)}{1+M}}-1. \tag{15}$$

Then, replacing G included in ε of equation (14) by G of equation (11), it yields

$$q_c=q_{c0}\left\{1+\frac{5}{6}\frac{0.0124+d/l}{(\rho_v/\rho_l)^{0.133}(\sigma\rho_l/G^2l)^{1/3}}\cdot\frac{\Delta H_i}{H_{fg}}\right\}.$$

Comparing this equation with equation (1) yields K in H-regime (designated by K_H) as follows:

$$K_H=\frac{5}{6}\frac{0.0124+d/l}{(\rho_v/\rho_l)^{0.133}(\sigma\rho_l/G^2l)^{1/3}}. \tag{16}$$

In Fig. 4, K_H predicted by equation (16) is compared with the experimental data of K_H compiled in Fig. 17 of the preceding study [3]. It may be concluded that agreement between predicted and measured K_H is fairly good.

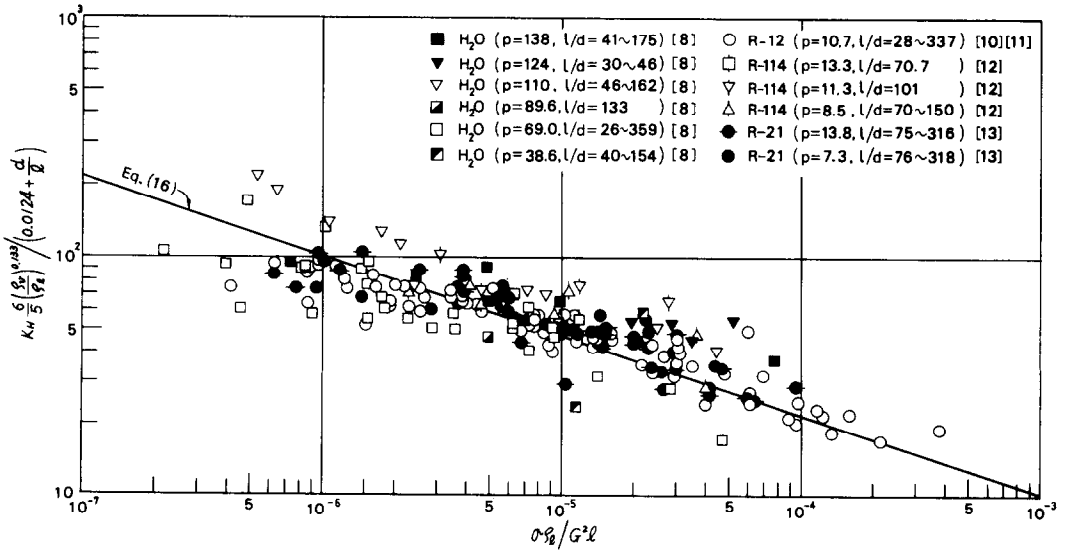

FIG. 4. Comparison between prediction of equation (16) and experimental data for K_H.

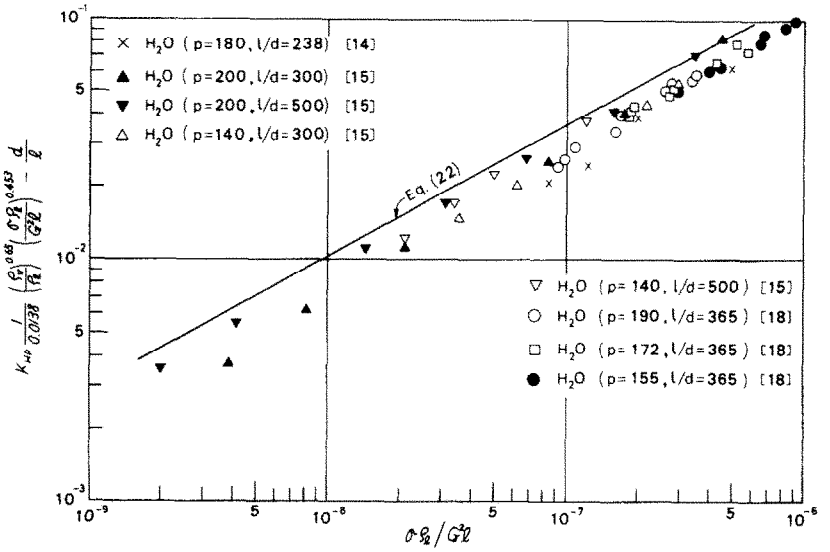

FIG. 5. Comparison between prediction of equation (22) and experimental data for K_{HP}.

4. PARAMETER K IN HP-REGIME

According to the author's correlation of q_{c0} [3], equations (2) and (4) are written for HP-regime as follows:

$$\frac{q_{c0}}{GH_{fg}} = 8.20\left(\frac{\rho_v}{\rho_l}\right)^{0.65}\left(\frac{\sigma\rho_l}{G^2 l}\right)^{0.453} \times \frac{1}{1+107(\sigma\rho_l/G^2 l)^{0.54} l/d} \quad (17)$$

$$\frac{q_c}{GH_{fg}} = 8.20\left(\frac{\rho_v}{\rho_l}\right)^{0.65}\left(\frac{\sigma\rho_l}{G^2 l_b}\right)^{0.453} \times \frac{1}{1+107(\sigma\rho_l/G^2 l_b)^{0.54} l_b/d}. \quad (18)$$

Then, in the same way as in the preceding section, the following equation is derived from equations (17), (18) and (3):

$$q_c(1-\varepsilon)^{0.453}\frac{1+N(1-\varepsilon)^{0.46}}{1+N} = q_{c0}, \quad (19)$$

where $N = 107(\sigma\rho_l/G^2 l)^{0.54} l/d$, and equation (19) can be replaced by

$$q_c\left\{1-\left(0.453+0.46\frac{N}{1+N}\right)\varepsilon\right\} = q_{c0} \quad (20)$$

with the relative error r defined as follows:

$$r = \frac{1-\left(0.453+0.46\dfrac{N}{1+N}\right)\varepsilon}{(1-\varepsilon)^{0.453}\dfrac{1+N(1-\varepsilon)^{0.46}}{1+N}} - 1. \quad (21)$$

Then, in the same way as before, equations (17), (20) and (1) yield K in HP-regime (designated by K_{HP}) as follows:

$$K_{HP} = 0.0138\frac{215(\sigma\rho_l/G^2 l)^{0.54} + d/l}{(\rho_v/\rho_l)^{0.65}(\sigma\rho_l/G^2 l)^{0.453}}. \quad (22)$$

It may be of interest to note that if d/l is removed from the RHS of equation (22), the equation is written as $K_{HP} = 2.97(\sigma\rho_l/G^2 l)^{0.087}/(\rho_v/\rho_l)^{0.65}$, which is nearly consistent with one of the equations of K_{HP} obtained empirically in the previous study [3], $K_{HP} = 3.08(\sigma\rho_l/G^2 l)^{0.09}/(\rho_v/\rho_l)^{0.6}$. Anyhow, in Fig. 5, K_{HP} predicted by equation (22) is compared with the experimental data of K_{HP} compiled in Fig. 18 of the preceding study [3]. The prediction of equation (22) is slightly higher than the experimental data, and it suggests that the correlation equation (17) may have a little defect with respect to the effect of l/d on CHF. At the present stage, however, the number of available data of q_{c0} in HP-regime is so limited that definite conclusions cannot be obtained.

5. PERMISSIBLE RANGE OF BOILING LENGTH METHOD

On the premise that the author's generalized correlation of q_{c0} [equations (5), (11) and (17)] is substantially valid, and that the linear $q_c - \Delta H_i$ relationship (Fig. 1) holds empirically in L-, H- and HP-regime, the results of Figs. 3–5 are regarded as showing the existence of a range in which the boiling length method for correlating CHF data is applicable with a permissible margin of error. It should be mentioned here that according to the existing CHF data (cf. Ref. [8] and others), the linear $q_c - \Delta H_i$ relationship can be observed to hold to the extent of $\varepsilon > 1$. Besides, logically speaking, it has been unnecessary in the present section to worry about the disagreement of flow pattern between the zero quality point in Fig. 2(a) and that in Fig. 2(b) and (c). Then, in compliance with a marginal magnitude of error, a permissible range of the boiling length method can be determined by equations (9), (15) and (21) for L-, H- and HP-regime respectively.

Numerical results thus obtained are shown in Tables 1–3, and it may be noticed that for the type of

Table 1. Permissible range of boiling length method in L-regime

$\lvert r\rvert < 0.025$	$\lvert r\rvert < 0.050$	$\lvert r\rvert < 0.100$
$-2.70 < \varepsilon^* < 0.59$	$-6.75 < \varepsilon^* < 0.69$	$-28.9 < \varepsilon^* < 0.79$

*r does not become positive for this range of ε.

Table 2. Permissible range of boiling length method in H-regime

M	$\lvert r\rvert < 0.025$	$\lvert r\rvert < 0.050$	$\lvert r\rvert < 0.100$
0.05	$-0.67 < \varepsilon^\dagger < 0.40$	$-1.06 < \varepsilon^\dagger < 0.52$	$-1.78 < \varepsilon^\dagger < 0.65$
0.15	$-0.92 < \varepsilon^\dagger < 0.44$	$-1.66 < \varepsilon^\dagger < 0.56$	$-4.27 < \varepsilon^\dagger < 0.68$
0.30	$-5.08 < \varepsilon < 0.52$	$-6.74 < \varepsilon < 0.63$	$-10.2 < \varepsilon < 0.74$
0.60	$-1.42 < \varepsilon < 0.72$	$-2.24 < \varepsilon < 0.78$	$-3.89 < \varepsilon < 0.85$
1.20	$-0.79 < \varepsilon^* < 0.47$	$-1.29 < \varepsilon^* < 0.62$	$-2.30 < \varepsilon^* < 0.80$
2.50	$-0.60 < \varepsilon^* < 0.35$	$-0.97 < \varepsilon^* < 0.45$	$-1.73 < \varepsilon^* < 0.57$
∞	$-0.45 < \varepsilon^* < 0.26$	$-0.73 < \varepsilon^* < 0.34$	$-1.30 < \varepsilon^* < 0.43$

*r does not become positive for this range of ε.
†r does not become negative for this range of ε.

Table 3. Permissible range of boiling length method in HP-regime

N	$\lvert r\rvert < 0.025$	$\lvert r\rvert < 0.050$	$\lvert r\rvert < 0.100$
0.50	$-0.69 < \varepsilon^* < 0.39$	$-1.12 < \varepsilon^* < 0.50$	$-1.94 < \varepsilon^* < 0.62$
1.00	$-0.79 < \varepsilon^* < 0.41$	$-1.31 < \varepsilon^* < 0.52$	$-2.39 < \varepsilon^* < 0.64$
2.00	$-0.92 < \varepsilon^* < 0.44$	$-1.59 < \varepsilon^* < 0.55$	$-3.09 < \varepsilon^* < 0.66$
5.00	$-1.11 < \varepsilon^* < 0.47$	$-2.01 < \varepsilon^* < 0.58$	$-4.25 < \varepsilon^* < 0.69$
∞	$-1.43 < \varepsilon^* < 0.51$	$-2.37 < \varepsilon^* < 0.62$	$-6.34 < \varepsilon^* < 0.73$

*r does not become negative for this range of ε.

Fig. 2(c), that is $\varepsilon < 0$, the range of ε for a fixed margin of error is comparatively wide in L-regime, whereas for the type of Fig. 2(b), that is $0 < \varepsilon < 1$, the range of ε for a fixed margin of error takes nearly the same value for L-, H- and HP-regime.

Supplementary note: N-regime

According to the preceding study [3], q_{c0} in N-regime is expressed as:

$$\frac{q_{c0}}{GH_{fg}} = 0.098\left(\frac{\rho_v}{\rho_l}\right)^{0.133}\left(\frac{\sigma\rho_l}{G^2 l}\right)^{0.433}\frac{(l/d)^{0.27}}{1+0.0031 l/d},$$

and the same procedure as that in Section 3 based on the boiling length concept provides the following equations instead of equations (15) and (16):

$$r = \frac{1-\left(0.163+\dfrac{M}{1+M}\right)\varepsilon}{(1-\varepsilon)^{0.163}\dfrac{1+M(1-\varepsilon)}{1+M}} - 1$$

$$K = 0.416\frac{(0.0221+d/l)(d/l)^{0.27}}{(\rho_v/\rho_l)^{0.133}(\sigma\rho_l/G^2 l)^{0.433}}.$$

On the other hand, however, it has been found in the preceding study [3] that linear $q_c - \Delta H_i$ relationship, that is equation (1), does not hold in N-regime. Therefore, it may be concluded that the boiling length concept is inapplicable in N-regime; and this character seems natural because CHF in N-regime is presumed to occur in a state very near zero quality.

6. TEST OF PERMISSIBLE RANGE OF BOILING LENGTH METHOD

6.1. *Experimental data*

In order to test the permissible range of the boiling length method predicted in Tables 1–3, experimental data of CHF obtained by Ueda *et al.* [16, 17] on R-113, Ueda [18] on R-113, Hynek *et al.* [19] on liquid nitrogen, and Bennett *et al.* [20] on water will be used. These experiments are concerned with the study of so-called dryout and post-dryout heat transfer, but no singular problems arise so long as the length of heated tube l used in this paper is measured as the distance between the entrance of the test tube and the dryout point which appears generally upstream from the exit of the test tube.

Table 4 lists main conditions of the experiments above-mentioned, including the experimental range of ε, l_b/l and M. Classification of experimental conditions into two regimes of L and H in Table 4 has been made in the following way. Namely, if it is tentatively assumed that the boiling length l_b is applicable for correlating CHF over the whole range of these experiments, experimental conditions can be plotted as in Figs. 6–8, where the boundary between adjoining regimes is given by the following equations derived by the author in previous studies [3,4]: for the boundary between L- and H-regime,

$$\frac{l_b}{d} = \frac{1}{0.10C(\rho_v/\rho_l)^{0.133}(\sigma\rho_l/G^2 l_b)^{0.29} - 0.0031}, \qquad (23)$$

where C takes the value indicated for equation (6), and for the boundary between H- and N-regime,

$$\frac{l_b}{d} = \frac{0.77}{(\sigma\rho_l/G^2 l_b)^{0.37}}. \quad (24)$$

In Figs. 6–8, experimental conditions located in and close to L-regime are indicated by open symbols, whereas those conditions located in H-regime by black symbols.

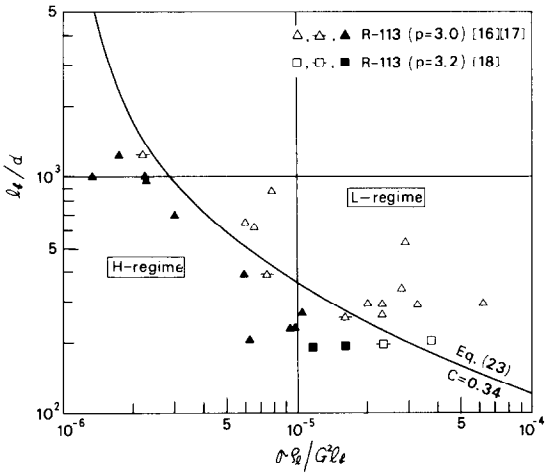

FIG. 6. Experimental conditions for R-113 [16–18].

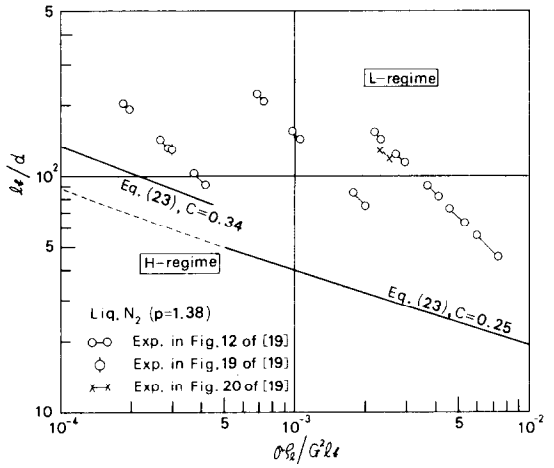

FIG. 7. Experimental conditions for liquid nitrogen [19].

6.2. *CHF in L-regime*

In Fig. 9, data of critical heat flux q_c obtained under the experimental conditions of open symbols are compared with the prediction of equation (6). The experimental data scatter to some extent, but it may be concluded that the data agree with the prediction of equation (6) based on the boiling length concept; and this result is regarded as reasonable because only minor errors are estimated by equation (9) within the experimental range of ε in L-regime indicated in Table 4.

Besides, it may be of interest to note in Fig. 9 that R-113 data ($p = 3.0$ bar) obtained by Ueda *et al.* [16, 17] for the type of Fig. 2(c) agree approximately with equation (6) for values of l_b/l extending from 14.06 to 2.50 (cf. Table 4). This may suggest that the flow in L-regime has a poor memory for the effect of upper stream and is governed by local conditions.

6.3. *CHF in H-regime*

In Fig. 10, data of critical heat flux q_c obtained for the experimental conditions in H-regime in Figs. 6–8 are compared with the prediction of equation (12). It may be noticed in Fig. 10 that the data obtained by Ueda *et al.* [16, 17] for the type of Fig. 2(c) suffer from scattering and have a trend to deviate from the prediction of equation (12), whereas the data obtained by Ueda [18] and Bennett *et al.* [19] for the type of Fig. 2(b) agree well with the prediction of equation (12). These results are consistent with the degree of error predicted by equation (15) for the experimental range of ε and M indicated in Table 4.

7. CONCLUSIONS

(i) The effect of inlet subcooling on CHF in L-, H- and HP-regime is analyzed, yielding equations (10), (16) and (22) to predict the parameter K in equation (1).

(ii) Fairly good agreement between the predicted and the measured K shown in Figs. 3–5 may be regarded as an indirect proof of the substantial validity of the author's generalized correlation of q_{c0}, that is, equations (5), (11) and (17).

(iii) The permissible range of the boiling length method is predicted by equations (9), (15) and (21) corresponding to a required magnitude of error.

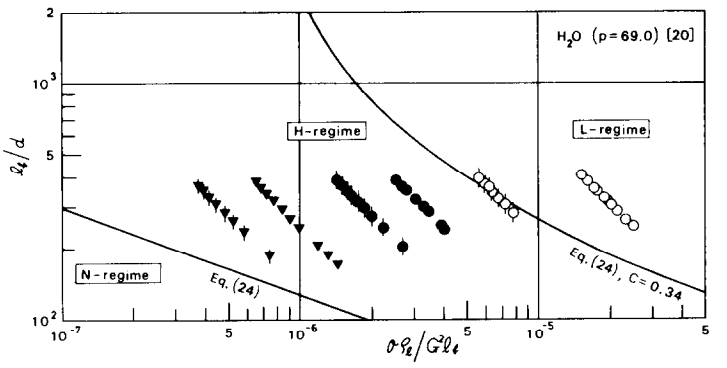

FIG. 8. Experimental conditions for water [20].

Table 4. Experimental range of ε, l_b/l, and M for data compared

Type		$\varepsilon < 0$		$0 < \varepsilon$	
Experiment		Ueda *et al.* [16, 17]	Ueda [18]	Hynek *et al.* [19]*	Bennett *et al.* [20]†
Fluid		R-113	R-113	Liq. N_2	H_2O
p (bar)		3.0	3.2	1.38	69.0
d (m)		0.01	0.01	0.0102	0.0126
L-regime	ε	$-13.06 \sim -1.50$	$0.174 \sim 0.197$	~ 0	$0.094 \sim 0.116$
	$\frac{l_b}{l}$	$14.06 \sim 2.50$	$0.826 \sim 0.803$	~ 1	$0.906 \sim 0.884$
H-regime	ε	$-23.73 \sim -3.95$	$0.216 \sim 0.231$	—	$0.101 \sim 0.166$
	$\frac{l_b}{l}$	$24.73 \sim 4.95$	$0.784 \sim 0.796$	—	$0.899 \sim 0.834$
	M	$0.0338 \sim 0.405$	0.760	—	$0.873 \sim 1.36$

*Data in Figs. 12, 19 and 20 of [19] are employed, excluding not only the data with tape, but also data of $G = 2 \times 10^4$ lb/ft^2 h in Fig. 20 because of VL-regime (cf. Ref. [3]).

†Data in Table 1 of [20] are employed, excluding data near N-regime ($G = 2.8 \times 10^6$ and 3.8×10^6 lb/ft^2 h).

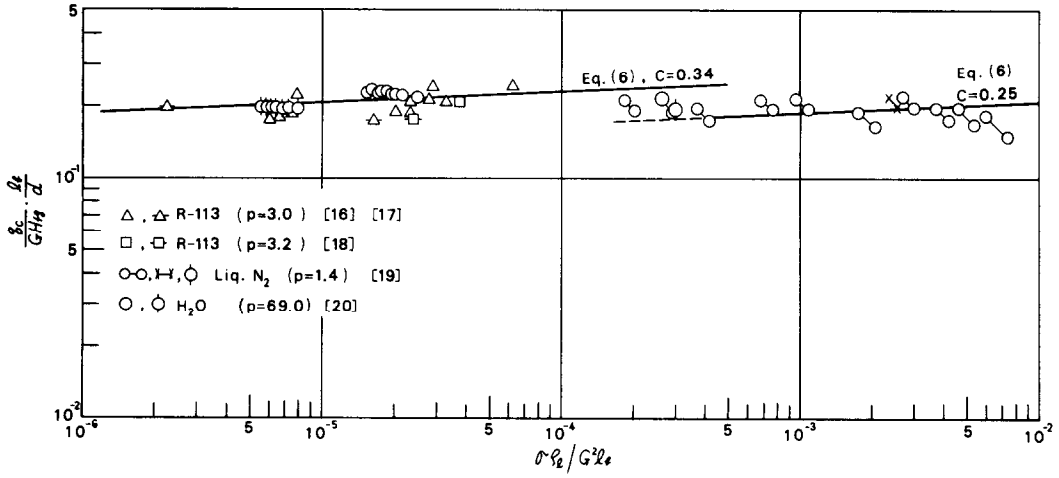

FIG. 9. Comparison between prediction of equation (6) and experimental data for CHF in L-regime.

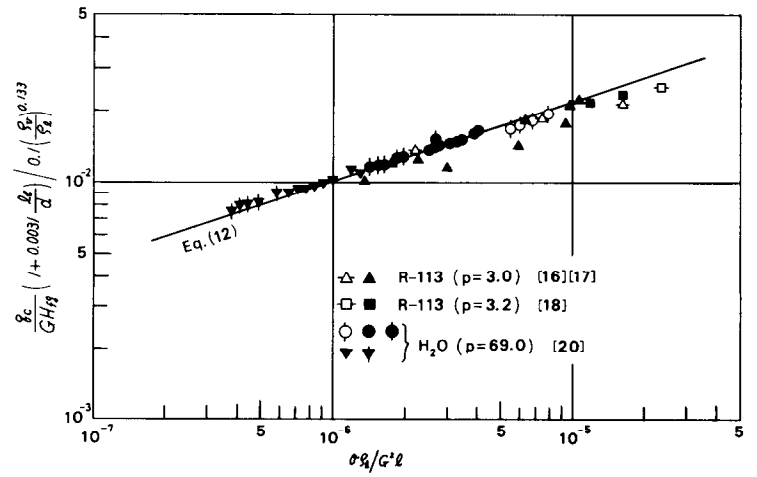

FIG. 10. Comparison between prediction of equation (12) and experimental data for CHF in H-regime.

(iv) When the inlet subcooling is within the permissible range of the boiling length method, the regime of CHF can be discriminated by employing the boiling length l_b instead of the heated length l [cf. equations (23) and (24)].

(v) According to the experimental data analyzed in the present paper, it seems likely that the flow in L-regime has a trend to establish it in a proper manner at every local position.

Acknowledgements—I would like to express my appreciation to the Ministry of Education, Science and Culture for support under Grant in Aid of Special Project Research No. 311602 (1978), and also to Professor T. Ueda for offering the important aid on CHF data.

REFERENCES

1. J. G. Collier, *Convective Boiling and Condensation*, p. 240. McGraw-Hill, New York (1972).
2. D. H. Lee, Prediction of Burnout, in *Two-phase Flow and Heat Transfer*, p. 296, Oxford University Press, Oxford (1977).
3. Y. Katto, A generalized correlation of critical heat flux for the forced convection boiling in vertical uniformly heated round tubes, *Int. J. Heat Mass Transfer* **21**, 1527 (1978).
4. Y. Katto, A generalized correlation of critical heat flux for the forced convection boiling in vertical uniformly heated round tubes—a supplementary report, *Int. J. Heat Mass Transfer* **22**, 783 (1979).
5. G. F. Hewitt, H. A. Kearsey, P. M. C. Lacey and D. J. Pulling, Burn-out and film flow in the evaporation of water in tubes, *Proc. Inst. Mech. Engrs* **180**(3C), 206 (1965–66).
6. S. Bertoletti, G. P. Gaspari, C. Lombardi, G. Peterlongo, M. Silverstri and F. A. Tacconi, Heat transfer crisis with steam–water mixtures, *Energ. Nucl.* **12**, 121 (1965).
7. V. Marinelli, Critical heat flux: a review of recent publications, *Nucl. Technol.* **34**, 135 (1977).
8. B. Thompson and R. V. Macbeth, Boiling water heat transfer burnout in uniformly heated round tubes: a compilation of world data with accurate correlations, U.K.A.E.A., AEEW-R 356 (1964).
9. W. H. Lowdermilk, C. D. Lanzo and B. L. Siegel, Investigation of boiling burnout and flow stability for water flowing in tubes, NACA TN 4382 (1958).
10. G. F. Stevens, D. F. Elliot and R. W. Wood, An experimental investigation into forced convection burnout in Freon, with reference to burn-out in water, uniformly heated round tubes with vertical up-flow, U.K. A.E.A., AEEW-R 321 (1964).
11. G. F. Stevens, D. F. Elliot and R. W. Wood, An experimental comparison between forced convection burn-out in Freon 12 flowing vertically upwards through uniformly and non-uniformly heated tubes, U.K.A.E.A., AEEW-R 426 (1965).
12. G. E. Dix, Freon–water modeling of CHF in round tubes, ASME-Paper No. 70-HT-26 (1970).
13. P. G. Barnett and R. W. Wood, An experimental investigation to determine the scaling laws of forced convection boiling heat transfer, Part 2, U.K.A.E.A., AEEW-R 443 (1965).
14. B. Chojnowski and P. W. Wilson, Critical heat flux for large diameter steam generating tubes with circumferentially variable and uniform heating, in *Proc. 5th Int. Heat Transfer Conference*, Vol. 4, p. 260. Hemisphere (1974).
15. K. M. Becker, D. Djursing, K. Lindberg, O. Eklind and C. Österdahl, Burnout conditions for round tubes at elevated pressures, in *Progress in Heat and Mass Transfer*, Vol. 6, p. 55. Pergamon Press, Oxford (1972).
16. T. Ueda, H. Tanaka and Y. Koizumi, Dryout of liquid film in high quality R-113 upflow in a heated tube, in *Proc. 6th Int. Heat Transfer Conference*, Vol. 1, p. 423. National Research Council of Canada (1978).
17. Y. Koizumi, T. Ueda and H. Tanaka, Post dryout heat transfer to R-113 upward flow in a vertical tube, *Int. J. Heat Mass Transfer* To be published.
18. T. Ueda, Personal communication.
19. S. J. Hynek, W. M. Rohsenow and A. E. Bergles, Forced-convection, dispersed-flow film boiling, Tech. Report No. 70586-63, MIT (1969).
20. A. W. Bennett, G. F. Hewitt, H. A. Kearsey and R. K. F. Keeys, Heat transfer to steam–water mixtures flowing in uniformly heated tubes in which the critical heat flux has been exceeded, U.K.A.E.A., AERE-R 5373 (1967).

ANALYSE DE L'EFFET DU SOUS-REFROIDISSEMENT A L'ENTREE SUR LE FLUX CRITIQUE EN EBULLITION AVEC CONVECTION FORCEE, DANS DES TUBES VERTICAUX ET UNIFORMEMENT CHAUFFES

Résumé—La formule généralisée du flux critique (CHF) obtenue par l'auteur dans des études précédentes est combinée avec le concept de longueur d'ébullition pour obtenir le calcul théorique de l'effet du sous-refroidissement à l'entrée sur le CHF. Un très bon accord est obtenu entre les estimations théoriques et les données de l'expérience. On examine quantitativement l'extension du sous-refroidissement d'entrée et de la méthode de la longueur d'ébullition applicable au calcul du CHF en comparant les données de CHF obtenues dans les études de l'assèchement et du transfert de chaleur après assèchement, avec la formule généralisée de l'auteur.

EINE UNTERSUCHUNG DES EINFLUSSES DER EINTRITTSUNTERKÜHLUNG AUF DIE KRITISCHE WÄRMESTROMDICHTE BEIM STRÖMUNGSSIEDEN IN SENKRECHTEN, GLEICHFÄRMIG BEHEIZTEN ROHREN

Zusammenfassung—Zur theoretischen Untersuchung des Einflusses der Eintrittsunterkühlung auf die kritische Wärmestromdichte (CHF) wird hier die vom Autor in früheren Untersuchungen hergeleitete verallgemeinerte Korrelation für CHF mit dem Konzept der Siede-Länge Kombiniert. Die Übereinstimmung der so gewonnenen Ergebnisse mit den vorhandenen experimentellen Daten ist leidlich gut. Ferner wird der Bereich der Eintrittsunterkühlung, in dem die Siede-Längen-Methode zur Berechnung von CHF-Werten anwendbar ist, quantitativ untersucht; hierzu werden CHF-Werte aus Wärmeübergangsuntersuchungen im dryout- und post-dryout-Gebiet mit der verallgemeinerten Korrelation des Autors verglichen.

АНАЛИЗ ВЛИЯНИЯ НЕДОГРЕВА НА ВХОДЕ ВЕРТИКАЛЬНЫХ РАВНОМЕРНО НАГРЕВАЕМЫХ ТРУБ НА КРИТИЧЕСКИЙ ТЕПЛОВОЙ ПОТОК ПРИ КИПЕНИИ В УСЛОВИЯХ ВЫНУЖДЕННОЙ КОНВЕКЦИИ

Аннотация — Для определения влияния недогрева на входе на критический тепловой поток (КТП) автор в данной статье использует понятие длины кипения и полученное им ранее обобщенное соотношение для КТП. Найденное таким образом соотношение хорошо описывает имеющиеся экспериментальные данные. Проведен количественный анализ степени недогрева на входе, для которой применим метод длины кипения, путём сравнения данных по КТП, полученных при исследовании так называемых критических и закритических режимов теплообмена, с обобщенным соотношением автора.